JACS
JOURNAL OF THE AMERICAN CHEMICAL SOCIETY

Article

pubs.acs.org/JACS

Uranyl and/or Rare-Earth Mellitates in Extended Organic–Inorganic Networks: A Unique Case of Heterometallic Cation–Cation Interaction with U^{VI}═O–Ln^{III} Bonding (Ln = Ce, Nd)

Christophe Volkringer, Natacha Henry, Stéphane Grandjean, and Thierry Loiseau*

Unité de Catalyse et Chimie du Solide (UCCS) – UMR CNRS 8181, Université de Lille Nord de France, USTL-ENSCL, Bat C7, BP 90108, 59652 Villeneuve d'Ascq, France, and Laboratoire de Chimie et Conversion des Actinides, CEA, DEN/DRCP/SCPS, Bât. 399, BP17171, 30208 Bagnols sur Cèze cedex, France

Supporting Information

ABSTRACT: A series of uranyl and lanthanide (trivalent Ce, Nd) mellitates (*mel*) has been hydrothermally synthesized in aqueous solvent. Mixtures of these 4f and 5f elements also revealed the formation of a rare case of lanthanide–uranyl coordination polymers. Their structures, determined by XRD single-crystal analysis, exhibit three distinct architectures. The pure lanthanide mellitate $Ln_2(H_2O)_6(mel)$ possesses a 3D framework built up from the connection of isolated $LnO_6(H_2O)_3$ polyhedra (tricapped trigonal prism) through the mellitate ligand. The structure of the uranyl mellitate $(UO_2)_3(H_2O)_6(mel)\cdot 11.5H_2O$ is lamellar and consists of 8-fold coordinated uranium atoms linked to each other through the organic ligand giving rise to the formation of a 2D 3^6 net. The third structural type, $(UO_2)_2Ln(OH)(H_2O)_3(mel)\cdot 2.5H_2O$, involves direct oxygen bondings between the lanthanide and uranyl centers, with the isolation of a heterometallic dinuclear motif. The 9-fold coordinated Ln cation, $LnO_5(OH)(H_2O)_3$, is linked to the 7-fold coordinated uranyl $(UO_2)O_4(OH)$ (pentagonal bipyramid) via one μ_2-hydroxo group and one μ_2-oxo group. The latter is shared between the uranyl bonding (U═O = 1.777(4)/1.779(6) Å) and a long Ln–O bonding (Ce–O = 2.822(4) Å; Nd–O = 2.792(6) Å). This unusual linkage is a unique illustration of the so-called cation–cation interaction associating 4f and 5f metals. The dinuclear motif is then further connected through the mellitate ligand, and this generates organic–inorganic layers that are linked to each other via discrete uranyl $(UO_2)O_4$ units (square bipyramid), which ensure the three-dimensional cohesion of the structure. The mixed U–Ln carboxylate is thermally decomposed from 260 to 280 °C and then transformed into the basic uranium oxide (U_3O_8) together with U–Ln oxide with the fluorite structural type ("$(Ln,U)O_2$"). At 1400 °C, only fluorite type "$(Ln,U)O_2$" is formed with the measured stoichiometry of $U_{0.63}Ce_{0.37}O_2$ and $U_{0.60}Nd_{0.40}O_{2-\delta}$.

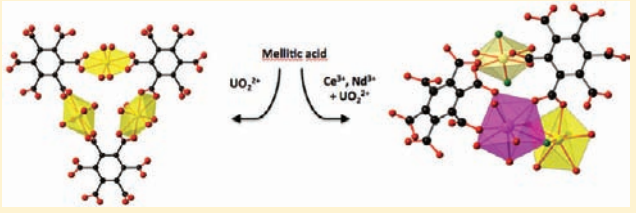

INTRODUCTION

In past decades, the research of hybrid materials combining metallic centers together with organic moieties has grown exponentially.[1] In this course, uranium was found to be a good candidate element for the generation of mixed organic–inorganic extended networks. When it is associated with multidentate O-donor ligands, such as carboxylate-based solids, uranium (especially with oxidation state VI) exhibits an interesting chemical ability to successfully form a wide variety of frameworks showing different dimensionalities.[2] In case of uranyl cation UO_2^{2+}, the possible coordination environments (4 + 2, square bipyramid; 5 + 2, pentagonal bipyramid; 6 + 2, hexagonal bipyramid)[3] also contribute to the richness of the structural topologies of such solids. The so-called uranyl–organic frameworks (UOF) have now been described in many contributions with the use of a large range of organic aliphatic[4] or aromatic[4j,5] carboxylates. Besides this class of compounds, tentative investigations have been carried out to combine metals from different blocks of the periodic table in such assemblies.[2b] Following this idea, there are rare few illustrations of mixed uranium–lanthanide carboxylates reported in the literature.[6] Most of the 4f–5f heretometallic complexes are based on the molecular assembly by mixing different functionalities of organic ligands with specific reactivities toward lanthanide or uranyl cations. In this way, lanthanide ions may interact through the N-donor organic functions, whereas the uranyl cations are preferentially bound to the O-donor part of the organic molecule. In other complexes, only O-donor interactions occur with either the lanthanide or the uranium centers. In all examples, the crystal structures are built up from the assemblage of discrete mononuclear motifs, without any direct chemical bonding between the 4f and 5f elements. The series of mixed uranium(IV)–lanthanides(III) oxalates constitutes another class of heterometallic extended networks.[7] It was shown that one given metal (5f or 4f) could be substituted by another one, on the same crystallographic position in a solid solution range for a given structural type. Here, oxalate moiety is a chelating agent, which has important applications in the liquid processes of nuclear industry. It can be used for the extraction of specific actinides

Received: October 21, 2011
Published: December 29, 2011

   dx.doi.org/10.1021/ja209915n | *J. Am. Chem.Soc.* 2012, 134, 1275–1283

and/or lanthanides, or further conversion of plutonium in the fabrication of MOX (UO_2/PuO_2 mixture) combustible. In this case, the use of lanthanide elements may simulate the chemical reactivity of the radionuclides plutonium or minor actinides. Alternatively, uranium carbide would be envisaged as potential fuel for the fourth generation of nuclear reactor.[8] Its dissolution in highly concentrated nitric acid solution was known to generate oxalate as well as mellitate species.[9] Mellitic acid (or 1,2,3,4,5,6-benzenehexacarboxylic acid, hereafter noted H_6mel) is an aromatic hexacarboxylate molecule, which has been used in the formation of extended networks involving magnetic cations,[10] for instance. Its reactivity toward rare-earth cations has been well documented in the literature,[10b,11] whereas only crystalline neptunium-based compounds[12] have been reported in the actinide family. With uranyl cations, one previous work mentioned the formation in aqueous solution of a complex "U_3mel_2", characterized by the spectrophotometric technique.[13]

This article deals with the hydrothermal reactivity of the mellitate anions toward uranyl and lanthanide cations. Only cerium and neodymium metals have been considered in this study because they usually play the role of surrogate elements for plutonium or americium (minor actinide), respectively. The lanthanide-based phases $Ln_2(H_2O)_6(mel)$ (Ce, **1**; Nd, **2**) and uranyl-based phase $(UO_2)_3(H_2O)_6(mel)\cdot 11.5H_2O$ (**3**) have been isolated. Regarding the comparison with the oxalate system, the tentative formation of mixed (Ce/Nd)−U mellitates has been envisaged. An unprecedented mixed cationic architecture has been observed in the phases $(UO_2)_2Ln(OH)(H_2O)_3(mel)\cdot 2.5H_2O$ (Ce, **4**; Nd, **5**), in which uranyl is directly bonded to lanthanide through oxygen atoms. Their synthesis conditions, structural descriptions (single-crystal X-ray diffraction), as well as the thermal behavior (TG, X-ray thermodiffraction, SEM for **4** and **5**) and spectroscopic measurements (IR, fluorescence for **3**−**5**) are presented.

EXPERIMENTAL SECTION

Synthesis. Caution! While uranyl nitrate $UO_2(NO_3)_2\cdot 6H_2O$ is a radioactive and chemically toxic reactant, precautions with suitable care and protection for handling such substances should be followed.

The metal mellitates have been hydrothermally synthesized under autogenous pressure using 23 mL Teflon-lined stainless steel Parr autoclave from the following reactants: cerium nitrate hexahydrate ($Ce(NO_3)_3\cdot 6H_2O$, Aldrich, 99%), neodymium nitrate hexahydrate ($Nd(NO_3)_3\cdot 6H_2O$, Aldrich, 99.9%), uranyl nitrate hexahydrate ($UO_2(NO_3)_2\cdot 6H_2O$, Merck 99%), mellitic acid (1,2,3,4,5,6-benzenehexacarboxylic acid or H_6mel, Aldrich, 99%), sodium hydroxide (NaOH, Aldrich, 98%), and deionized water. The starting chemical reactants are commercially available and have been used without any further purification. Phases **4** and **5** were obtained pure, whereas **1** and **2** were produced during synthesis trials of **4** and **5**, typically without NaOH (which is used for pH modification). Phase **3** was obtained during our investigations in preparing phase **5**, and NaOH concentrations differ between the two syntheses. It was noted that phase **3** could not be obtained in the absence of neodymium cations. The latter remained soluble because no neodymium mellitate crystallite is visible after the hydrothermal reaction.

*$Ce_2(H_2O)_6(mel)$ (**1**).* A mixture of 502 mg (1 mmol) of $UO_2(NO_3)_2\cdot 6H_2O$, 218 mg (0.5 mmol) of $Ce(NO_3)_3\cdot 6H_2O$, 85 mg (0.25 mmol) of mellitic acid, and 5 mL (277 mmol) of H_2O was placed in a Parr autoclave and then heated statically at 200 °C for 24 h. The resulting product showing a mixture of **1** (colorless crystallites) and **4** (orange crystallites) was then filtered off, washed with water, and dried at room temperature.

*$Nd_2(H_2O)_6(mel)$ (**2**).* A mixture of 502 mg (1 mmol) of $UO_2(NO_3)_2\cdot 6H_2O$, 200 mg (0.5 mmol) of $Nd(NO_3)_3\cdot 6H_2O$, 85 mg (0.25 mmol) of mellitic acid, and 5 mL (277 mmol) of H_2O was placed in a Parr autoclave and then heated statically at 200 °C for 24 h. The resulting product showing a mixture of **2** (purple crystallites) and **5** (yellow crystallites) was then filtered off, washed with water, and dried at room temperature.

*$(UO_2)_3(H_2O)_6(mel)\cdot 11.5H_2O$ (**3**).* A mixture of 502 mg (1 mmol) of $UO_2(NO_3)_2\cdot 6H_2O$, 200 mg (0.45 mmol) of $Nd(NO_3)_3\cdot 6H_2O$, 85 mg (0.25 mmol) of mellitic acid, 0.1 mL (0.1 mmol) of NaOH (1 M), and 5 mL (277 mmol) of H_2O was placed in a Parr autoclave and then heated statically at 200 °C for 24 h. The resulting yellow product was then filtered off, washed with water, and dried at room temperature. It gave needle-like crystallites with specific hexagonal shape of 80−400 μm as it can be observed by SEM (Figure 1). One observed that the blocks consisted of the stacking of thin plates (thickness ≈ 1−10 μm), perfectly aligned along a hexagonal axis.

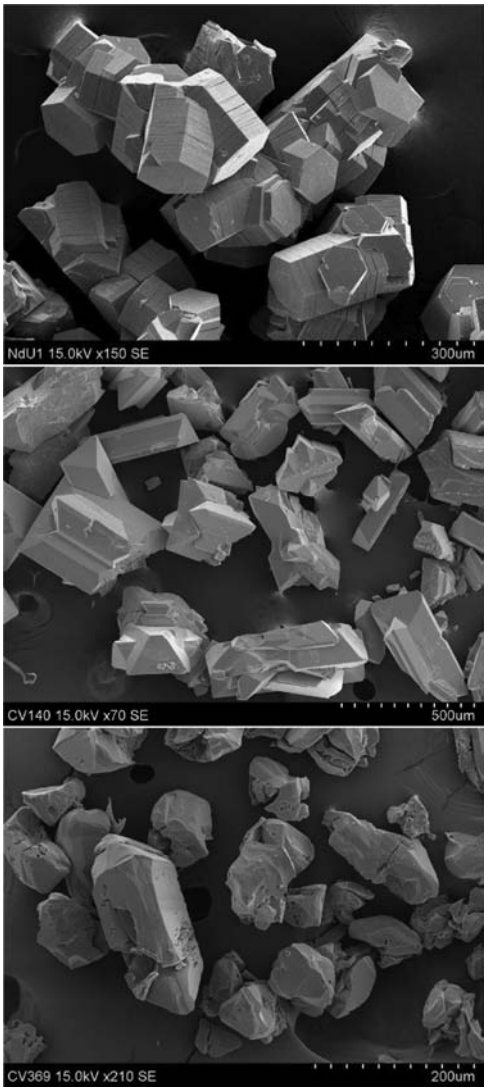

Figure 1. SEM images of the as-synthesized compounds **3** (top), **4** (middle), and **5** (bottom).

*$Ce(UO_2)_2(OH)(H_2O)(mel)_2$ (**4**).* A mixture of 502 mg (1 mmol) of $UO_2(NO_3)_2\cdot 6H_2O$, 218 mg (0.5 mmol) of $Ce(NO_3)_3\cdot 6H_2O$, 85 mg (0.25 mmol) of mellitic acid, 0.3 mL (1.2 mmol) of NaOH (4 M), and 5 mL (277 mmol) of H_2O was placed in a Parr autoclave and then heated statically at 200 °C for 24 h. The resulting orange product was then filtered off, washed with water, and dried at room temperature. It gave crystallites with a specific block shape of 80−400 μm as it can be observed by SEM (Figure 1).

dx.doi.org/10.1021/ja209915n | J. Am. Chem.Soc. 2012, 134, 1275−1283

Table 1. Crystal Data and Structure Refinements for Mellitates

	1	3	4	5
formula	$C_{12}H_{12}Ce_2O_{18}$	$C_{12}O_{31}U_3$	$C_{12}H_{12}CeO_{22.5}U_2$	$C_{12}H_{12}NdO_{22.5}U_2$
formula weight	724.46	1354.2	1132.40	1136.52
temperature/K	293(2)	293(2)	293(2)	293(2)
crystal type	colorless block	yellow needle	orange block	yellow needle
crystal size/mm	0.14 × 0.13 × 0.05	0.12 × 0.08 × 0.04	0.14 × 0.13 × 0.07	0.35 × 0.11 × 0.11
crystal system	orthorhombic	trigonal	orthorhombic	orthorhombic
space group	*Pnnm*	*P*-3*m*1	*Pnma*	*Pnma*
a/Å	13.5874(3)	11.5310(3)	15.5887(5)	15.578(3)
b/Å	6.7390(1)	11.5310(3)	11.6182(3)	11.628(2)
c/Å	10.2833(2)	6.8198(2)	13.1134(3)	13.065(3)
α/deg	90	90	90	90
β/deg	90	90	90	90
γ/deg	90	120	90	90
volume/Å^3	941.60	785.30(4)	2375.0(1)	2366.5(1)
Z, $\rho_{calculated}$/g cm^{-3}	2, 2.484	1, 2.863	4, 3.167	4, 3.190
μ/mm^{-1}	4.871	15.541	15.592	15.918
Θ range/deg	3.01−30.76	2.04−36.32	2.03−30.54	2.03−27.95
limiting indices	$-19 \le h \le 18$	$-19 \le h \le 19$	$-22 \le h \le 22$	$-20 \le h \le 18$
	$-8 \le k \le 9$	$-18 \le k \le 19$	$-16 \le k \le 16$	$-15 \le k \le 15$
	$-14 \le l \le 14$	$-11 \le l \le 11$	$-18 \le l \le 18$	$-17 \le l \le 17$
collected reflections	14 626	39 530	108 050	40 785
unique reflections	1515 [R(int) = 0.0337]	1428 [R(int) = 0.0329]	3799 [R(int) = 0.0557]	2912 [R(int) = 0.0585]
parameters	97	25	181	181
GOF on F^2	1.115	5.46	1.203	1.230
final R indices [$I > 2\sigma(I)$]	R1 = 0.0174	R1 = 0.0450	R1 = 0.0252	R1 = 0.0291
	wR2 = 0.0429	wR2 = 0.0788	wR2 = 0.0713	wR2 = 0.0793
R indices (all data)	R1 = 0.0198	R1 = 0.0478	R1 = 0.0289	R1 = 0.0337
	wR2 = 0.0441	wR2 = 0.08792	wR2 = 0.0811	wR2 = 0.0907
largest diff. peak and hole/e Å^{-3}	0.672 and −1.004	4.80 and −2.68	2.662 and −1.125	2.419 and −1.571

*$Nd(UO_2)_2(OH)(H_2O)(mel)_2$ (**5**).* A mixture of 502 mg (1 mmol) of $UO_2(NO_3)_2{\cdot}6H_2O$, 300 mg (0.68 mmol) of $Nd(NO_3)_3{\cdot}6H_2O$, 85 mg (0.25 mmol) of mellitic acid, 0.15 mL (0.6 mmol) of NaOH (4 M), and 5 mL (277 mmol) of H_2O was placed in a Parr autoclave and then heated statically at 200 °C for 24 h. The resulting yellow product was then filtered off, washed with water, and dried at room temperature. It gave crystallites with specific block shape of 30−180 μm as it can be observed by SEM (Figure 1).

Single-Crystal X-ray Diffraction. Crystals were easily selected under polarizing optical microscope and glued on a glass fiber for a single-crystal X-ray diffraction experiment. X-ray intensity data were collected on a Bruker X8-APEX2 CCD area-detector diffractometer using Mo K_α radiation (λ = 0.71073 Å) with an optical fiber as collimator. Several sets of narrow data frames (20 s per frame) were collected with ω scans. Data reduction was accomplished using SAINT V7.53a.[14] The substantial redundancy in data allowed a semiempirical absorption correction (SADABS V2.10[15]) to be applied, on the basis of multiple measurements of equivalent reflections. The structure was solved by direct methods, developed by successive difference Fourier syntheses, and refined by full-matrix least-squares on all F^2 data using JANA2006[16] program. The final refinements include anisotropic thermal parameters of all non-hydrogen atoms. For phase **3**, SEM analysis (Figure 1) clearly indicated the stacking of thin plates forming the hexagonal crystallites, which may give rise to twinned crystal issues. The merged reflections in monoclinic, orthorhombic, trigonal, or hexagonal yield R_{int} factors between 3.16% and 3.42%. In the absence of systematic extinctions, the highly symmetric first space group, *P*6/*mmm*, was considered. The structure solution obtained using superflip software[17] was refined to R1 = 6.99%. Surprisingly, all of the oxygen atoms were disordered on two positions. Lower symmetries were then tested, and a reasonable model was obtained with *P*-3*m*1 together with the twin law (−100/0−10/001) even if a water molecule remains disordered (R1 = 4.5%). The crystal data are given in Table 1. Supporting Information is available in CIF format.

Thermogravimetric Analysis. The thermogravimetric experiments have been carried out on a thermoanalyzer TGA 92 SETARAM under air atmosphere with a heating rate of 5 °C.min^{-1} from room temperature to 800 °C. X-ray thermodiffractometry was performed under 5 L h^{-1} air flow in an Anton Paar HTK1200N of a D8 Advance Bruker diffractometer (θ−θ mode, Cu Kα radiation) equipped with a Vantec1 linear position sensitive detector (PSD). Each powder pattern was recorded in the range 5−60° (2θ) (at intervals of 20 °C to 800 °C) with a 0.5 s/step scan, corresponding to an approximate duration of 30 mn. The temperature ramps between two patterns were 0.08 °C s^{-1} to 800 °C. The as-synthesized complexes were also placed in a platinum crucible and heated in a furnace in air atmosphere at different temperatures (800, 1000, 1200, and 1400 °C).

Infrared Spectroscopy. Infrared spectra of compounds **3**−**5** were measured on Perkin-Elmer Spectrum Two spectrometer between 4000 and 400 cm^{-1}, equipped with a diamond attenuated total reflectance (ATR) accessory (see the Supporting Information).

Fluorescence. Fluorescence spectra of the powdered compounds **3**−**5** were measured at room temperature on SAFAS FLX-Xenius spectrometer between 400 and 800 nm, equipped with a xenon lamp. The fluorescence spectrum of uranyl dinitrate hexahydrate, $UO_2(NO_3)_2{\cdot}6H_2O$, was also presented for comparison (see the Supporting Information).

RESULTS

Structure Description. *Crystal Structure of $Ce_2(H_2O)_6$(mel) (**1**).* The compounds **1** and **2** have identical structures, related to that of a lanthanum-based phase. The latter was first mentioned by Williams et al.,[11c] who reported the synthesis of a series of rare-earth mellitates with similar orthorhombic symmetry (S.G. *Pnnm*) for larger cations from La to Er. The La-based structure[11c] as well as the Nd- and Ho-based structures[11f]

dx.doi.org/10.1021/ja209915n | J. Am. Chem.Soc. 2012, 134, 1275−1283

have been previously determined by X-ray diffraction, and we briefly describe the crystal structure of the Ce (**1**) analogous compound. It has a three-dimensional network, based on one rare-earth cation lying on a special position *4g* (mirror plane). The metal is 9-fold coordinated with three terminal aquo groups and six carboxyl oxygen atoms belonging to four distinct mellitate ligands. The resulting coordination polyhedron is a distorted tricapped trigonal prism, $CeO_6(H_2O)_3$. The Ce−O distances range from 2.392(2) to 2.636(2) Å for Ce (**1**). The Ce−OH_2 distances are 2.503(2) and 2.600(2) Å. The discrete motifs $CeO_6(H_2O)_3$ are connected to each other through all of the carboxylate arms of the mellitate anions. Four of the six carboxylate groups adopt a chelating connection mode with the cationic centers and link four $CeO_6(H_2O)_3$ polyhedra in the (*a*,*c*) plane, whereas the two remaining ones adopt a bidentate bridging with two adjacent metal centers along the *c* axis (Figure 2).

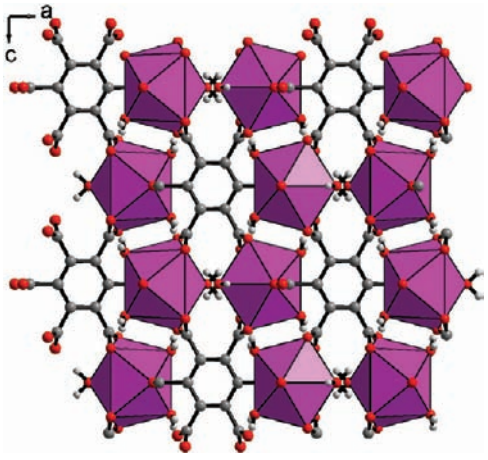

Figure 2. View of the structure $Ln_2(mel)(H_2O)_6$ (Ln = Ce (**1**), Nd (**2**)) showing the connection of the mellitate anions with the discrete $LnO_6(H_2O)_3$ polyhedra along the *c* axis.

The resulting framework is quite compact, and narrow channels are observed along the *c* axis, and delimited by terminal water molecules. A similar three-dimensional network was recently described by Thuéry and Masco[18] with the aliphatic version of the cyclic hexacarboxylate assembled with europium cations.

*Crystal Structure of $(UO_2)_3(H_2O)_6(mel)\cdot 11.5H_2O$ (**3**).* The structural analysis reveals that one independent uranium center (Figure 3) is 8-fold coordinated to four carboxyl oxygen atoms (U−O = 2.481(10) Å), two oxygen atoms from the typical uranyl bonds (U═O = 1.770(14) Å), and two water molecules in terminal position (U−Ow1 = 2.36(2) Å). The assignment of terminal aquo group agrees with the bond valence calculations.[19] The IR frequency of the double uranyl bond is observed at 916 cm^{-1} and assigned to its antisymmetric vibration ν_3 (see the Supporting Information). Following the empirical relationship given by Bartlett and Cooney,[20] the estimation of the uranyl bond length is calculated to be 1.773 Å and fits well with the experimental value from single-crystal XRD analysis. The structure model shows that the uranium-centered hexagonal bipyramids are linked to each other through all of the carboxylate arms of the mellitate molecule around the hexagonal axis of its benzene ring. Each carboxylate group adopts a chelating connection mode with uranium, occupying a trans position in the hexagonal equatorial plane of the coordination polyhedron. Such a configuration was previously reported in literature for discrete 8-fold coordinated uranyl units.[4f,i,j,5b−d,j,21]

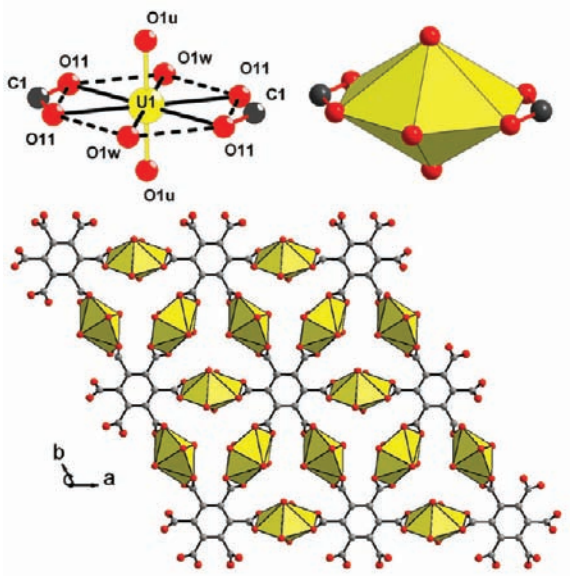

Figure 3. (top) Representation of the 8-fold coordination environment of the uranyl cation in $(UO_2)_3(H_2O)_6(mel)\cdot nH_2O$ (**3**). (bottom) View of a layer along the *c* axis, showing the connection of the hexagonal bipyramids $(UO_2)O_4(H_2O)_2$ with the mellitate linker to generate a 3^6 net.

It generates layers with a 3^6 net topology (Figure 3), if one considers aromatic rings as nodes of triangles and uranium-centered polyhedra forming its edges. The mellitate molecule acts as a hexadentate ligand linking six uranium cations. Hydration water molecules are disorderly located between the mixed organic−inorganic layers, which are stacked along the *c* axis. Thermogravimetric analysis (Supporting Information) indicated the removal of water between room temperature and 150 °C, with an estimated amount of $11.5H_2O$ per $(UO_2)_3$ unit. The product was transformed into α-U_3O_8 (pdf file 047-1493) from 560 °C (see X-ray thermodiffraction in the Supporting Information). The fluorescence spectrum (Supporting Information) of **3** exhibited quite unresolved bands with the most intense peaks positioned at 499.4, 533.4, and 597.0 nm.

*Crystal Structures of $(UO_2)_2Ln(OH)(H_2O)_3(mel)\cdot 2.5H_2O$ (Ln = Ce (**4**), Nd (**5**)).* Compounds **4** and **5** exhibit unusual structural features for crystal chemistry of uranyl-based solids. First, they are rare examples of heterometallic compounds, in which both hexavalent uranyl and trivalent lanthanide cations are chemically bonded. Indeed, one uranyl cation (U1) occupies one crystallographic site (special position *4c*, mirror plane symmetry) and is 7-fold coordinated with a typical pentagonal bipyramidal configuration (Figure 4). As expected for uranium(VI), two double uranyl bonds exist with typical short U═O distances (U1−O1 = 1.765(5) or 1.750(7) Å for **4** and **5**, respectively; U1−O2 = 1.777(4) and 1.779(6) Å for **4** and **5**, respectively). The five oxygen atoms of the pentagonal equatorial plane have U−O distances ranging from 2.251(5) to 2.426(3) Å, and 2.258(6) to 2.426(4) Å for **4** and **5**, respectively. Four of these oxygen atoms are shared with carboxylate groups of the mellitate linkers. The remaining oxygen atom (O1H), which has a shorter U−O distance (~2.25 Å), is bridging a lanthanide center (Ce or Nd) and corresponds to a μ_2-hydroxo group (in agreement with bond valence summations,[19,22] with values of 1.18 for **4** and 1.16 for **5**). The cerium or neodymium cation is bound to nine oxygen atoms in a distorted tricapped trigonal prismatic coordination sphere (Figure 4).

dx.doi.org/10.1021/ja209915n | *J. Am. Chem.Soc.* 2012, 134, 1275−1283

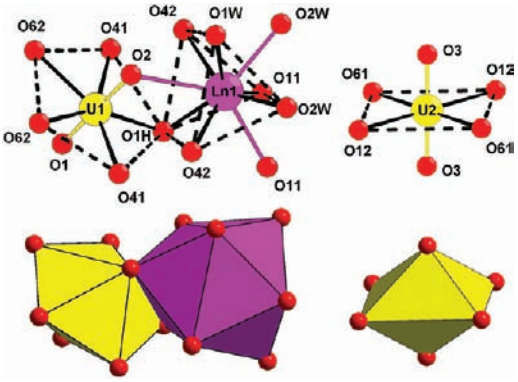

Figure 4. (left) Views of the mixed U–(Ce/Nd) dinuclear brick $(UO_2)(OH)O_8Ln(H_2O)_3$ showing the 7-fold coordinated uranyl cation (U1) linked to the 9-fold coordinated rare-earth metal centers via uranyl oxo species (O2) and equatorial hydroxo species (O1H) in $(UO_2)_2Ln(OH)(H_2O)_3(mel)\cdot 2.5H_2O$ (Ce (**4**), Nd (**5**)). Dotted line indicated pentagonal plane for uranyl U1 and trigonal prism for Ln1. Yellow bonds correspond to the typical uranyl double bonds (O1, O2), whereas purple bonds are between Ln1 and oxo or terminal aquo species capping the square faces of the trigonal prismatic polyhedron. (right) Views of the 6-fold coordinated uranyl cation U2, involved in a square plane bipyramidal polyhedron $(UO_2)O_4$. Yellow bonds correspond to the typical uranyl double bonds (O3).

Apart from the hydroxo group (Ce–O1H = 2.411(5) Å; Ce–O1H = 2.378(6) Å), four of the oxygen atoms belong to carboxylate groups of mellitate, and three oxygen atoms are terminal aquo species. Typical Ln–O distances in the range 2.494(6)–2.554(4) Å for **4** and 2.466(7)–2.523(5) Å for **5** are observed for these trivalent rare-earth metals. The last remaining atom O2, which is involved in the uranyl bond attached to uranium U1, is also considered in the coordination environment of the lanthanide and characterized by a much longer Ln–O distance (Ce1–O2 = 2.822(4) Å and Nd1–O2 = 2.792(6) Å). Calculated bond valence[22] value is 0.16 for O2 from the contribution of the Ln–O bond. This unprecedented U=O–Ln linkage slightly affects the uranyl bond distance, with deviations of +0.012 Å (**4**) and +0.029 Å (**5**) as compared to the second terminal U=O bond (with O1). This type of connection involving a uranyl μ_2-oxo group is related to the rare examples of the so-called cation–cation interactions (CCIs) occurring in pure hexavalent uranyl compounds.[5l,23] An increase of the U=O bond length was usually observed up to ~+0.05 Å[23h] for this specific configuration. It is slightly higher than that of the mixed U=O–Ln bonding in **4** and **5**. This is certainly due to the fact of longer metal–oxygen bonds for cerium or neodymium as compared to the uranium–oxygen ones. The double uranyl bond was analyzed by infrared spectroscopy in the region 950–800 cm^{-1} related to the antisymmetric vibrations (ν_3). Two bands are observed at 932 and 912 cm^{-1} for **4** and 928 and 917 cm^{-1} for **5** (Supporting Information). Tentative assignments following the Bartlett and Cooney[20] empirical law $[d(U{=}O)_{(pm)} = 9141(\nu_{3(cm-1)})^{-2/3} + 80.4]$ led to the U1 crystallographic site for vibrations at 906 or 917 cm^{-1}, and crystallographic site U2 for vibrations at 932 or 928 cm^{-1}. Calculated uranyl bond lengths from the IR frequency values give U1=O, 1.776 Å (XRD: 1.765(5) and 1.750(7) Å) for **4**; U1=O, 1.772 Å (XRD: 1.777(4) and 1.779(6) Å) for **5**; U2=O, 1.762 Å (XRD: 1.756(4) Å) for **4**; and U2=O, 1.765 Å (XRD: 1.763(5) Å) for **5**. The two cationic centers are also linked through two carboxylate arms of two distinct mellitate molecules. To our knowledge, no such hetero metallic bonding involving 4f–5f elements was previously reported in the literature related to extended coordination polymers, involving O-donor ligands. However, a very recent contribution of Arnold and co-workers has shown such cation–cation interaction between pentavalent uranyl and trivalent samarium or yttrium elements by using N-donor macrocycle molecules favoring the formation of molecular bimetallic species.[24] The heterodinuclear units containing the $(UO_2)O_4(OH)$ and $LnO_5(OH)(H_2O)_3$ polyhedra are further connected to each other via the carboxylate groups of mellitate in a bidentate bridging mode (via O41 and O42; positions 1,4 of the benzene ring) along the *b* axis and monodentate briding mode along the *c* axis (via O62 and O11; positions 2,3,5,6 of the benzene ring). It results in the generation of mixed organic–inorganic sheets developing in the (*b*,*c*) plane (Figure 5). Whereas the bidentate carboxylate arms

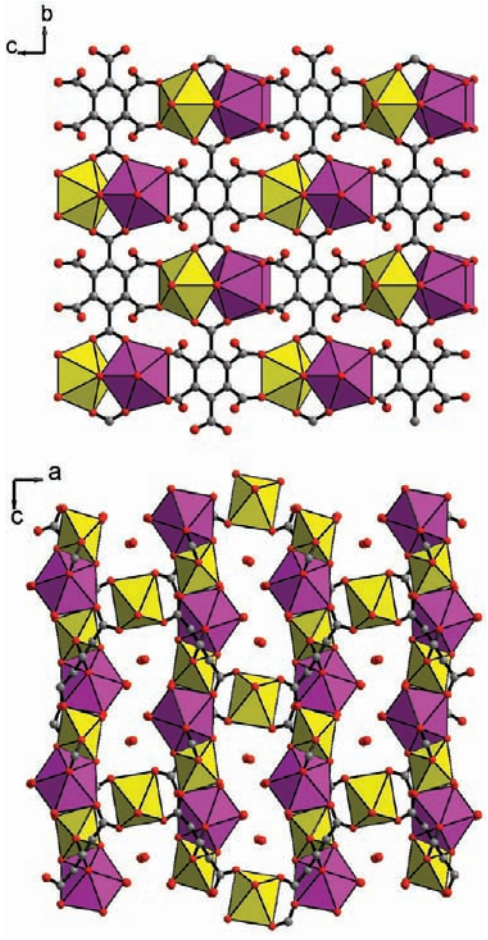

Figure 5. (top) View of the layer in $(UO_2)_2Ce(OH)(H_2O)_3(mel)\cdot 2.5H_2O$ (Ce (**4**), Nd (**5**)) perpendicular to the *a* axis. (bottom) View of the 3D framework of **4** and **5** along the *b* axis, showing the connection of layers to each other through discrete 6-fold coordinated uranyl cation U2.

are located along the (*b*,*c*) plane, the monodentate carboxylate ones are twisted, and the remaining nonbonded carboxyl oxygen atoms are pointed upward or downward the (*b*,*c*) layer. The latter are connected to a second uranyl moiety (U2), located on the special position *4a* (inversion center). This uranium U2 is 6-fold coordinated in a square bipyramidal environment. Besides the two terminal uranyl oxygen atoms found at 1.756(4) Å

dx.doi.org/10.1021/ja209915n | J. Am. Chem.Soc. 2012, 134, 1275–1283

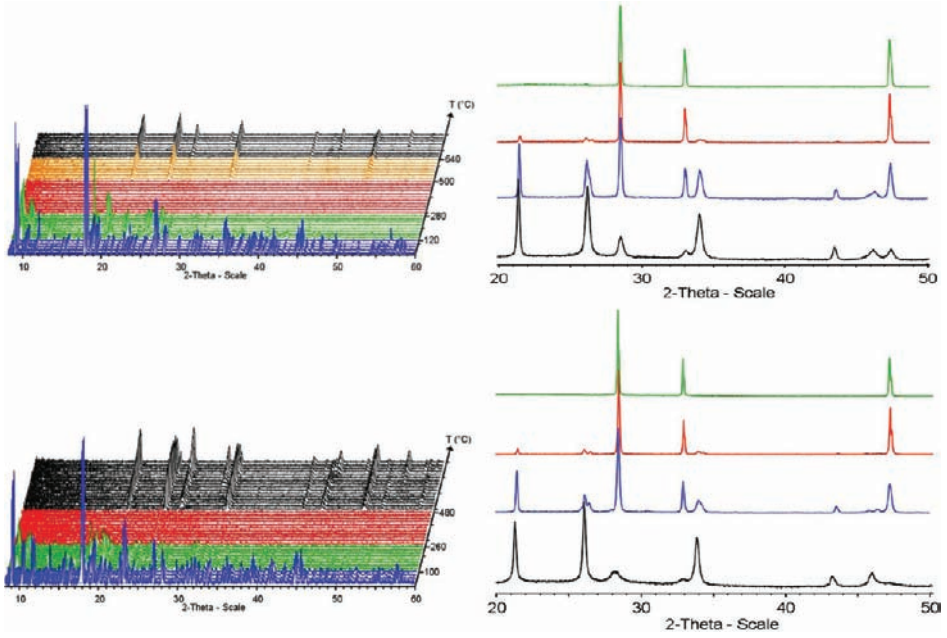

Figure 6. Right: X-ray thermodiffractograms of $(UO_2)_2Ce(OH)(H_2O)_3(mel)\cdot 2.5H_2O$ (**4**, top) and $(UO_2)_2Nd(OH)(H_2O)_3(mel)\cdot 2.5H_2O$ (**5**, bottom) (copper radiation). Left: X-ray diffractograms of **4** (top) and **5** (bottom), collected after calcination at 800 °C (black), 1000 °C (blue), 1200 °C (red), and 1400 °C (green) showing the disappearance of U_3O_8 at the benefit of "$(U,Ln)O_2$" fluorite-type oxide.

(**4**) and 1.763(5) Å (**5**) from the uranium atom U2, four other oxygen atoms are engaged with the non bonded carboxylate arm of the mellitate and perpendicularly placed in a square plane with U−O distances of 2.365(3) and 2.384(3) Å, and 2.363(4) and 2.378(4) Å, for **4** and **5**, respectively. The existence of such a 6-fold surrounding for uranyl cation is the second original structural characteristic for this structure. In most of the structures, uranium(VI) is found in 7- or 8-fold surrounding, with either pentagonal or hexagonal plane perpendicularly to the double uranyl bonds. For instance, Burns reported some examples of purely inorganic compounds[3] in which such an isolated square bipyramidal surrounding occurs for uranyl, but it is rarely reported in coordination complexes.[5a,23b,25] This discrete $(UO_2)O_4$ unit plays the role of pillar between the mixed layers containing mellitates and heterometallic dimers and ensures the three-dimensional character of the structure (Figure 5). Identical $(UO_2)O_4$ connecting block was encountered in uranyl phosphates[26] or vanadates.[27] The mellitate molecule acts as an octadentate ligand, linking four distinct dinuclear units and four isolated mononuclear units. A similar connection mode is also found in the lanthanide-based compounds **1** and **2**, in which one organic ligand links eight distinct Ln-centered polyhedral motifs. The framework reveals puckered channels running along the *b* axis and encapsulating free statistically disordered water molecules. The latter interact through hydrogen-bond interactions with the terminal aquo species attached to the rare-earth cation (O2W···O3W ≈ 2.99 Å; O2W···O5W ≈ 2.99 Å; O1W···O4W ≈ 2.74 Å). The fluorescence spectra of compounds **4** and **5** are quite identical but rather complex and unresolved (Supporting Information). The most intense broad band is located at 529.4 nm for **4** and 536.4 nm for **5**. They are both red-shifted (+21.4/+28.4 nm) as compared to the fluorescence spectrum of uranyl nitrate hexahydrate.

Thermal Behavior. The thermal stability and decomposition of the mixed uranyl−lanthanide compounds **4**, **5** have been studied by thermogravimetric analysis and X-ray thermodiffraction.

The thermogravimetric curve (Supporting Information) of **4** indicates a continuous weight loss up to 260 °C (10.0%), followed by two plateaus up to 310 and 385 °C (7.4%). The final weight loss is 36.3%. Considering the final formation of basic oxides $(2/3)U_3O_8$ and CeO_2, the calculated remaining loss is 64.8% as compared to the observed value (obs: 63.7%). It is quite difficult to assign the weight losses of the different chemical components of the compound (hydroxo, aquo groups, or organic linker) due to the observation of the continuous loss event. The observed weight loss between 300 and 380 °C could be tentatively assigned to one step of decarboxylation ($-2CO_2$ at 380 °C, calcd 7.1%; obs 7.4%). The content of trapped water molecules is also quite delicate to estimate because only a continuous weight loss is visible between room temperature and 250 °C. However, the final weight loss is compatible with the chemical formula deduced from single-crystal X-ray diffraction analysis. The X-ray thermodiffraction (Figure 6) shows Bragg peaks of the compounds **4** up to 280 °C, with intensities change from 120 °C, which could be correlated to the departure of free water molecules within the cavities. After 280 °C, the compound is decomposed and then transformed into α'-U_3O_8 (pdf file 31-1425) from 500 °C. From 640 °C, a second phase crystallizes and is assigned to CeO_2 (pdf file 65-5923) with the cubic fluorite type.

The thermogravimetric curve (Supporting Information) of the neodymium analogue (**5**) exhibits a continuous weight loss up to 500 °C. The final weight loss is 34.7% and corresponds to the decomposition of the compound into the basic oxides U_3O_8 and $(Nd,U)O_{2-\delta}$ (see thermodiffractogram in Figure 6). Tentative assignments could be done as follows: the free water is evacuated up to 120 °C (obs 4.0%, calcd 3.6%). A step between 250 and 370 °C could be attributed to the partial decarboxylation of the linker (ex: $-1CO_2$, obs 3.6%; calcd 3.9%). However, due to the absence of plateaus, such accurate attributions remain quite delicate. The X-ray thermodiffraction diagram (Figure 6) is quite similar to that of the cerium analogue. The Bragg peaks of the compounds **5** are visible up to 260 °C, with intensities changing

dx.doi.org/10.1021/ja209915n | *J. Am. Chem.Soc.* 2012, 134, 1275−1283

from 100 °C, related to the departure of free water molecules. After its degradation, two distinct oxides crystallize from 480 °C, with the formation of uranium oxide U_3O_8 (α and α' forms, pdf files 31-1424 and 31-1425) and a neodymium−uranium oxide $(Nd,U)O_{2-\delta}$ (pdf file 75-0090) with the cubic fluorite type.

The calcination (in air) of the as-synthesized compounds **4** and **5** was then analyzed by XRD and SEM. Evolution of the XRD patterns between 800 and 1400 °C shows the progressive disappearance of the uranium oxide U_3O_8. At 1400 °C, only the mixed fluorite phase "$(Ce,U)O_2$" or "$(Nd,U)O_{2-\delta}$" is visible. The final compositions are $Ce_{0.63}U_{0.37}O_2$ and $U_{0.60}Nd_{0.40}O_{2-\delta}$ (from EDS analysis), which is close that of the as-synthesized phase (2U/1Ln). For both compounds, the SEM photographs of the calcined solids at 800 °C show cracked crystallites of 10−120 μm size, reminiscent of the parallelepiped-like morphology of the as-synthesized phases, obtained after hydrothermal treatment (Figure 7 for **4**, see Supporting Information for **5**).

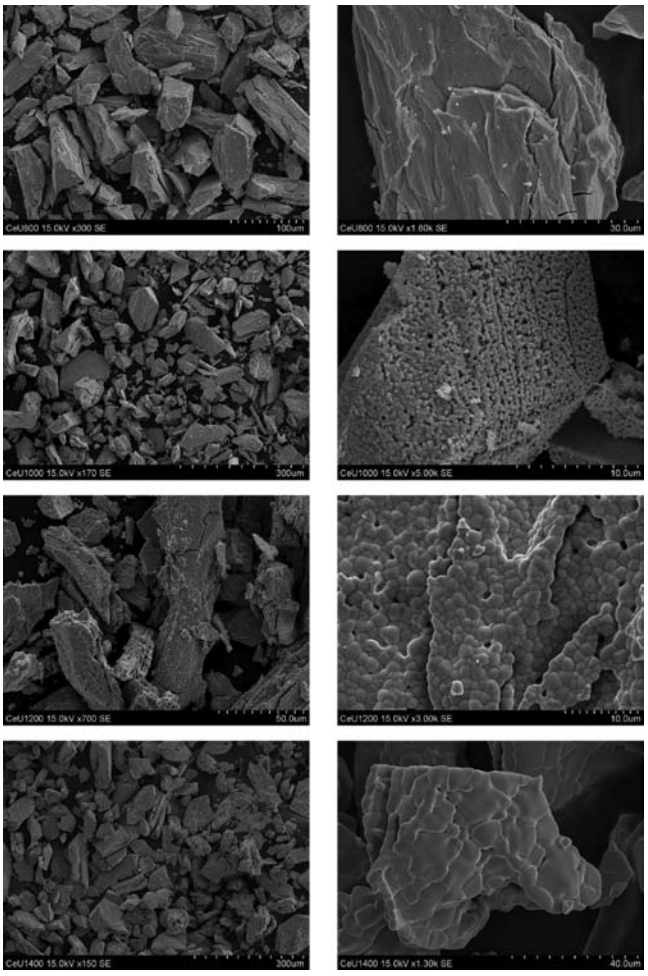

Figure 7. SEM images of the calcined crystallites of **4** after heating at 800, 1000, 1200, and 1400 °C (from top to bottom), under air for 24 h. (left) Views of crystallites morphology; (right) detailed views of crystallites surface. SEM images of the calcined compound **5** are presented in the Supporting Information.

Whereas the morphology of the crystallites does not change so much at a higher temperature, crystal growth of the final phase "$(U,Ln)O_2$" with the fluorite type is clearly visible at its surface, with flat grain size varying from 0.1 to 0.2 μm at 1000 °C to 10−30 μm at 1400 °C. Such flat crystalline microscopic domains have been previously reported in the case of hyperstoichiometic UO_{2+x}.[28]

CONCLUSION

The hydrothermal reactivity of the hexacarboxylate mellitate ligand has been investigated with aqueous solutions containing lanthanide (such as Ce^{3+} or Nd^{3+}) and uranyl cations. A series of solids $Ln_2(H_2O)_6(mel)$ (Ln = Ce, Nd), with a known structural type (previously reported with La,[11c] Nd,[11f] Ho[11f]), has been synthesized and consists of isolated tricapped trigonal prismastic polyhedra, $LnO_6(H_2O)_3$, engaged with the octadendate mellitate anions in a three-dimensional framework. A uranyl mellitate, $(UO_2)_3(H_2O)_6(mel)\cdot 11.5H_2O$, has also been isolated and exhibits a layered structure containing 8-fold coordinated uranium atoms connected to each other through the organic linkers, to generate a 3^6 net. Water molecules are intercalated between the mixed organic−inorganic sheets. This compound is a new example of actinide mellitate because only neptunium-based solids[12] have been identified so far. A third type of compounds also crystallizes under this hydrothermal condition and concerns a distinct architecture, $(UO_2)_2Ln(OH)(H_2O)_3(mel)\cdot 2.5H_2O$ (Ln = Ce, Nd), involving both cations 4f and 5f. They can be obtained as pure phases with the addition of the inorganic base NaOH (molar NaOH/U = 1.2), for instance. The rare-earth atom is still 9-fold coordinated ($LnO_5(OH)(H_2O)_3$), but linked to a neighboring 7-fold coordinated uranyl cation $(UO_2)O_4(OH)$ via μ_2-hydroxo and μ_2-oxo bridges. The latter anion belongs to the typical short uranyl bonding. The layers generated from the connection of heterometallic dinuclear units with mellitate ligands are further linked to each other via isolated $(UO_2)O_4$ square bipyramidal motifs to form the three-dimensional structure. Indeed, these mixed uranyl−lanthanide mellitates exhibit new structural features. This is a unique case of heterometallic bonding between uranyl and lanthanide elements, which corresponds to a novel illustration of the cation−cation interaction. This type of μ_2-oxo bridge has been rarely reported in pure uranyl-based compounds,[23h,i] because the usual terminal "yl" oxygen is quite chemically inert[29] for further condensation processes with other metallic centers. A second μ_2-hydroxo linkage is also observed between the two metals 4f and 5f, and this has not been previously reported in other coordination complexes. The rare-earth and uranyl cations are generally associated through the connection of different organic ligands, with assemblies involving covalent bondings and/or hydrogen-bond interactions.[6a−c,e−h] No direct U═O−Ln bonding is reported in coordination complexes with hexavalent uranyl. Yet, a case of a molecular biheterometallic U═O−Sm (or Y) species stabilized N-donor macrocycles recently was discovered by Arnold et al.[24] and involved pentavalent uranium. Nevertheless, such a linkage was, for instance, described in the natural mineral Bijvoetite,[30] for which the 8-fold coordinated uranyl polyhedra share a common μ_2-oxo edge with the 8-fold coordinated lanthanide polyhedra in a carbonate-based layer. The thermal degradation of the mixed Ln−U mellitates led to the formation of a mixture of basic uranium oxide (U_3O_8) and mixed Ln−U oxide "$(Ln,U)O_2$" crystallizing with the fluorite structural type. Above 1000 °C, uranium oxide U_3O_8 progressively disappears, and only the fluorite type compound is visible. Final compositions of the mixed solids at 1400 °C were $Ce_{0.63}U_{0.37}O_2$ and $Nd_{0.60}U_{0.40}O_{2-\delta}$. The SEM analysis of the surface of the as-synthesized crystallites clearly shows the growth of crystalline flat domains related to the fluorite phase when heated above 1000 °C.

dx.doi.org/10.1021/ja209915n | J. Am. Chem.Soc. 2012, 134, 1275−1283

■ ASSOCIATED CONTENT

Supporting Information

Optical microscope images of **3**−**5**, powder XRD patterns of **3**−**5**, crystallographic data for **1**, **3**−**5** (cif files), IR and fluorescence spectra of **3**−**5**, TG curves of **3**−**5**, X-ray thermodiffraction of **3**, and SEM images of calcination of **5**. This material is available free of charge via the Internet at http://pubs.acs.org.

■ AUTHOR INFORMATION

Corresponding Author

thierry.loiseau@ensc-lille.fr

■ ACKNOWLEDGMENTS

We would like to thank the GNR MATINEX of PACEN interdisciplinary program and the French ANR project no. ANR-08-BLAN-0216-01 for financial support. We also would like to thank Pr. Francis Abraham (UCCS) and Dr. Philippe Moisy (CEA) for helpful discussions, Pr. Marielle Huvé for the EDS analysis, and Nora Djelal and Laurence Burylo for technical assistance with the SEM images, TG measurements, and powder XRD (UCCS).

■ REFERENCES

(1) See themed issue, Metal−Organic Frameworks: *Chem. Soc. Rev.* **2009**, *38*, 1201.

(2) (a) Leciejewicz, J.; Alcock, N. W.; Kemp, T. J. *Struct. Bonding (Berlin)* **1995**, *82*, 43. (b) Cahill, C. L.; de Lill, D. T.; Frisch, M. *CrystEngComm* **2007**, *9*, 15. (c) Wang, K.-X.; Chen, J.-S. *Acc. Chem. Res.* **2011**, *44*, 531.

(3) Burns, P. C. *Can. Mineral.* **2005**, *43*, 1839.

(4) (a) Benetollo, F.; Bombieri, G.; Herrero, J. A.; Rojas, R. M. *J. Inorg. Nucl. Chem.* **1979**, *41*, 195. (b) Bombieri, G.; Benetollo, F.; Del Pra, A.; Rojas, R. M. *J. Inorg. Nucl. Chem.* **1979**, *41*, 201. (c) Borkowski, L. A.; Cahill, C. L. *Cryst. Growth Des.* **2006**, *6*, 2241. (d) Borkowski, L. A.; Cahill, C. L. *Cryst. Growth Des.* **2006**, *6*, 2248. (e) Borkowski, L. A.; Cahill, C. L. *Acta Crystallogr., Sect. E* **2005**, *61*, m816. (f) Borkowski, L. A.; Cahill, C. L. *Inorg. Chem.* **2003**, *42*, 7041. (g) Thuéry, P. *CrystEngComm* **2009**, *11*, 232. (h) Thuéry, P. *Eur. J. Inorg. Chem.* **2006**, 3646. (i) Thuéry, P.; Masci, B. *Cryst. Growth Des.* **2008**, *8*, 3430. (j) Thuéry, P. *Cryst. Growth Des.* **2011**, *11*, 347.

(5) (a) Cousson, A.; Proust, J.; Pagès, M. *Acta Crystallogr., Sect. C* **1990**, *46*, 2316. (b) Cousson, A.; Stout, B. E.; Necroux, E.; Pagès, M.; Gasperin, M. *J. Less-Common Met.* **1986**, *125*, 111. (c) Kim, J.-Y.; Norquist, A. J.; O'Hare, D. *Dalton Trans.* **2003**, 2813. (d) Go, Y. B.; Wang, X.; Jacobson, A. J. *Inorg. Chem.* **2007**, *46*, 6594. (e) Charushnikova, I. A.; Krot, N. N.; Polyakova, I. N.; Makarenkov, V. I. *Radiochemistry* **2005**, *47*, 241. (f) Charushnikova, I. A.; Krot, N. N.; Starikova, Z. A. *Radiochemistry* **2004**, *46*, 556. (g) Liao, Z.-L.; Li, G.-D.; Wei, X.; Yu, Y.; Chen, J.-S. *Eur. J. Inorg. Chem.* **2010**, 3780. (h) Borkowski, L. A.; Cahill, C. L. *Acta Crystallogr., Sect. E* **2004**, *60*, m198. (i) Thuéry, P. *Inorg. Chem. Commun.* **2008**, *11*, 616. (j) Thuéry, P. *CrystEngComm* **2009**, *11*, 1081. (k) Mihalcea, I.; Henry, N.; Loiseau, T. *Cryst. Growth Des.* **2011**, *11*, 1940. (l) Mihalcea, I.; Henry, N.; Clavier, N.; Dacheux, N.; Loiseau, T. *Inorg. Chem.* **2011**, 6243.

(6) (a) Rojas, R. M.; Herrero, M. P.; Benetollo, F.; Bombieri, G. *J. Less-Common Met.* **1990**, *162*, 105. (b) Pons y Moll, O.; Le Borgne, T.; Thuéry, P.; Ephritikine, M. *Acta Crystallogr., Sect. C* **2001**, *57*, 392. (c) Leverd, P. C.; Rinaldo, D.; Nierlich, M. *J. Chem. Soc., Dalton Trans.* **2002**, 829. (d) Schelter, E. J.; Veauthier, J. M.; Thompson, J. D.; Scott, B. L.; John, K. D.; Morris, D. E.; Kiplinger, J. L. *J. Am. Chem. Soc.* **2006**, *128*, 2198. (e) Thuéry, P. *CrystEngComm* **2008**, *10*, 1126. (f) Thuéry, P. *Inorg. Chem.* **2009**, *48*, 825. (g) Thuéry, P. *Cryst. Growth Des.* **2010**, *10*, 2061. (h) Thuéry, P. *CrystEngComm* **2009**, *11*, 2319.

(7) (a) Chapelet-Arab, B.; Nowogrocki, G.; Abraham, F.; Grandjean, S. *J. Solid State Chem.* **2005**, *178*, 3046. (b) Chapelet-Arab, B.; Nowogrocki, G.; Abraham, F.; Grandjean, S. *J. Solid State Chem.* **2005**, *178*, 3055. (c) Chapelet-Arab, B.; Duvieubourg, L.; Nowogrocki, G.; Abraham, F.; Grandjean, S. *J. Solid State Chem.* **2006**, *179*, 4029.

(8) (a) Guérin, Y.; Was, G. S.; Zinkle, S. J. *MRS Bull.* **2009**, *34*, 10. (b) A Technology Roadmap for Generation IV Nuclear Energy Systems (http://www.gen-4.org/PDFs/GenIVRoadmap.pdf, accessed Jan 2010), issued by D.O.E. and Generation IV forum, 2002.

(9) Ferris, L. M.; Bradley, M. J. *J. Am. Chem. Soc.* **1965**, *87*, 1710.

(10) (a) Humphrey, S. M.; Mole, R. A.; Thompson, R. I.; Wood, P. T. *Inorg. Chem.* **2010**, *49*, 3441. (b) Taylor, K. M. L.; Jin, A.; Lin, W. *Angew. Chem., Int. Ed.* **2008**, *47*, 7722.

(11) (a) Wu, L. P.; Munakata, M.; Kuroda-Sowa, T.; Maekawa, M.; Suenaga, Y. *Inorg. Chim. Acta* **1996**, *249*, 183. (b) Wu, L. P.; Munakata, M.; Yamamoto, M.; Kuroda-Sowa, T.; Maekawa, M. *J. Coord. Chem.* **1996**, *37*, 361. (c) Chui, S. S.-Y.; Siu, A.; Feng, X.; Zhang, Z. Y.; Mak, T. C. W.; Williams, I. D. *Inorg. Chem. Commun.* **2001**, *4*, 467. (d) Deluzet, A.; Guillou, O. *Acta Crystallogr., Sect. C* **2003**, *59*, m277. (e) Li, Z.-F.; Wang, C.-X.; Wang, P.; Zhang, Q.-H. *Acta Crystallogr., Sect. E* **2006**, *62*, m914. (f) Tang, X.; Yue, S.; Li, P.; Wang, N.; Liu, Y. *J. Rare Earths* **2008**, *26*, 800.

(12) (a) Nectoux, F.; Abazli, H.; Jové, J.; Cousson, A.; Pagès, M.; Gasperin, M.; Choppin, G. *J. Less-Common Met.* **1984**, *97*, 1. (b) Cousson, A.; Dabos, S.; Abazli, H.; Nectoux, F.; Pagès, M.; Choppin, G. *J. Less-Common Met.* **1984**, *99*, 233.

(13) Hasilkar, S. P.; Kamat, J. V.; Chander, K.; Marathe, S. G. *Radiochem. Radiation Chem. Symp., Kampur (India)* **1985**, 429.

(14) *SAINT Plus Version 7.53a*; Bruker Analytical X-ray Systems: Madison, WI, 2008.

(15) Sheldrick, G. M. *SADABS, Bruker-Siemens Area Detector Absorption and Other Correction, Version 2008/1*; Bruker: Madison, WI, 2008.

(16) Petricek, V.; Dusek, M.; Palatinus, L. *JANA2006. Structure determination software programs*; Institute of Physics: Praha, Czech Republic, 2006.

(17) (a) van Smaalen, S.; Palatinus, L.; Schneider, M. *Acta Crystallogr., Sect .A* **2003**, *59*, 459. (b) Palatinus, L.; Chapuis, G. *J. Appl. Crystallogr.* **2007**, *40*, 786.

(18) Thuéry, P.; Masco, B. *Cryst. Growth Des.* **2010**, *10*, 3626.

(19) Burns, P. C.; Ewing, R. C.; Hawthorne, F. C. *Can. Mineral.* **1997**, *35*, 1551.

(20) Bartlett, J. R.; Cooney, R. P. *J. Mol. Struct.* **1989**, *193*, 295.

(21) (a) Xia, Y.; Wang, K.-X.; Chen, J.-S. *Inorg. Chem. Commun.* **2010**, *13*, 1542. (b) Liao, Z.-L.; Li, G.-D.; Bi, M.-H.; Chen, J.-S. *Inorg. Chem.* **2008**, *47*, 4844. (c) Thuéry, P. *Cryst. Growth Des.* **2011**, *11*, 2606.

(22) Brese, N. E.; O'Keeffe, M. *Acta Crystallogr., Sect. B* **1991**, *47*, 192.

(23) (a) Taylor, J. C.; Ekstrom, A.; Randall, C. H. *Inorg. Chem.* **1978**, *17*, 3285. (b) Thuéry, P.; Nierlich, M.; Souley, B.; Asfari, Z.; Vicens, J. *Dalton Trans.* **1999**, 2589. (c) Rose, D.; Chang, Y.-D.; Chen, Q.; Zubieta, J. *Inorg. Chem.* **1994**, *33*, 5167. (d) Brandenburg, N. P.; Loopstra, B. O. *Acta Crystallogr., Sect. B* **1978**, *34*, 3734. (e) Sullens, T. A.; Jensen, R. A.; Shvareva, T. Y.; Albrecht-Schmitt, T. E. *J. Am. Chem. Soc.* **2004**, *126*, 2676. (f) Kubatko, K.-A.; Burns, P. C. *Inorg. Chem.* **2006**, *45*, 10277. (g) Lhoste, J.; Henry, N.; Roussel, P.; Loiseau, T.; Abraham, F. *Dalton Trans.* **2011**, *40*, 2422. (h) Krot, N. N.; Grigoriev, M. S. *Russ. Chem. Rev.* **2004**, *73*, 89. (i) Fortier, S.; Hayton, T. W. *Coord. Chem. Rev.* **2010**, *254*, 197. (j) Morrison, J. M.; Moore-Shay, L. J.; Burns, P. C. *Inorg. Chem.* **2011**, *50*, 2272. (k) Siegel, S.; Viste, A.; Hoekstra, H. R.; Tani, B. *Acta Crystallogr., Sect. B* **1972**, *28*, 117. (l) Taylor, J. C.; Wilson, P. W. *Acta Crystallogr., Sect. B* **1973**, *29*, 1073. (m) Alekseev, E. V.; Krivovichev, S. V.; Malcherek, T.; Depmeier, W. *Inorg. Chem.* **2007**, *46*, 8442. (n) Alekseev, E. V.; Krivovichev, S. V.; Depmeier, W.; Siidra, O. I.; Knorr, K.; Sulaimanov, E. V.; Chuprunov, E. V. *Angew. Chem., Int. Ed.* **2006**, *45*, 7233. (o) Alekseev, E. V.; Krivovichev, S. V.; Depmeier, W. *J. Solid State Chem.* **2009**, *182*, 2977. (p) Krivovichev, S. V. *Radiochemistry* **2008**, *50*, 450. (q) Obbade, S.; Dion, C.; Rivenet, M.; Saadi, M.; Abraham, F. *J. Solid State Chem.* **2004**, *177*, 2058. (r) Obbade, S.; Duvieubourg, L.; Dion, C.; Abraham,

F. *J. Solid State Chem.* **2007**, *180*, 866. (s) Obbade, S.; Renard, C.; Abraham, F. *J. Solid State Chem.* **2009**, *182*, 413. (t) Renard, C.; Obbade, S.; Abraham, F. *J. Solid State Chem.* **2009**, *182*, 1377. (u) Severance, R. C.; Smith, M. D.; zur Loye, H.-C. *Inorg. Chem.* **2011**, *50*, 7931.
(24) Arnold, P. L.; Hollis, E.; White, F. J.; Magnani, N.; Caciuffo, R.; Love, J. B. *Angew. Chem., Int. Ed.* **2011**, *50*, 887.
(25) Rowland, C. E.; Belai, N.; Knope, K. E.; Cahill, C. L. *Cryst. Growth Des.* **2010**, *10*, 1390.
(26) (a) Demartin, F.; Diella, V.; Donzelli, S.; Gramaccioli, C. M.; Pilati, T. *Acta Crystallogr., Sect. B* **1991**, *47*, 439. (b) Danis, J. A.; Runde, W. H.; Scott, B.; Fettinger, J.; Eichhorn, B. *Chem. Commun.* **2001**, 2378.
(27) Jouffret, L.; Shao, Z.; Rivenet, M.; Abraham, F. *J. Solid State Chem.* **2010**, *183*, 2290.
(28) He, H.; Shoesmith, D. *Phys. Chem. Chem. Phys.* **2010**, *12*, 8108.
(29) Gordon, G.; Taube, H. *J. Inorg. Nucl. Chem.* **1961**, *19*, 189.
(30) Li, Y.; Burns, P. C.; Gault, R. A. *Can. Mineral.* **2000**, *38*, 153.